

Analyst

Accepted Manuscript



This is an *Accepted Manuscript*, which has been through the Royal Society of Chemistry peer review process and has been accepted for publication.

Accepted Manuscripts are published online shortly after acceptance, before technical editing, formatting and proof reading. Using this free service, authors can make their results available to the community, in citable form, before we publish the edited article. We will replace this *Accepted Manuscript* with the edited and formatted *Advance Article* as soon as it is available.

You can find more information about *Accepted Manuscripts* in the [Information for Authors](#).

Please note that technical editing may introduce minor changes to the text and/or graphics, which may alter content. The journal's standard [Terms & Conditions](#) and the [Ethical guidelines](#) still apply. In no event shall the Royal Society of Chemistry be held responsible for any errors or omissions in this *Accepted Manuscript* or any consequences arising from the use of any information it contains.

Cite this: DOI: 10.1039/c0xx00000x

www.rsc.org/xxxxxx

ARTICLE TYPE

Stimulated mass enhancement strategy-based highly sensitive detection of a protein in serum using quartz crystal microbalance technique†

Rashida Akter, Bongjin Jeong and Md. Aminur Rahman *

Received (in XXX, XXX) Xth XXXXXXXXXX 20XX, Accepted Xth XXXXXXXXXX 20XX

DOI: 10.1039/b000000x

A stimulated mass enhancement strategy based on enormous biocatalytic precipitations of 4-chloro-1-naphthol (CN) using magnetic bead (MB)-supported horseradish peroxidase (HRP) and glucose oxidase (GOx) bienzymes was developed for the highly sensitive detection of interleukin-6 (IL-6) in serum using quartz crystal microbalance (QCM) technique.

The sensitive detection of protein biomarkers in real serum samples plays an important role for diagnosing diseases at an early state. Conventional immunoassay methods for proteins detection in serum include enzyme-linked immunosorbent assay (ELISA),¹ radioimmunoassay (RIA),² fluorescence,³ chemiluminescence,⁴ electrophoretic,⁵ and mass spectrometric immunoassays⁶ suffers from drawbacks: time-consuming, radiation hazards, tedious, expensive, need for skilled personnel, and sophisticated instrumentation. As alternatives to the conventional immunoassay procedures, immunosensor methods based on surface plasma resonance (SPR),⁷ chemiluminescence,⁸ electrochemistry⁹ and quartz crystal microbalance (QCM),¹⁰ have been developed for the protein detection. Of these, the QCM

immunosensors have shown great promises as the real-time and label-free detection can be achieved with a high sensitivity and specificity. The QCM measure the decrease in resonant frequency, f_0 (Δf), which linearly depends on the mass attached to the quartz crystal surface according to the Sauerbrey relationship,¹¹

$$\Delta f = -2 \Delta m f_0^2 / [A(\mu_q \rho_q)^{1/2}] \quad (1)$$

where Δf is the change in frequency (Hz), Δm is the mass change (g), n is the overtone number, A is the area of the quartz crystal, μ_q is the shear modulus of the quartz (2.947×10^{11} g/(cm·sec²)), and ρ_q is the density of the quartz (2.648 g/cm³), assuming the attached mass is rigid and strongly coupled to the resonator. The Sauerbrey equation does not apply for viscoelastic mass, therefore its analytical application is originally limited for the precise mass detection in liquid phase. However, it is reported that for a high frequency quartz (~10 MHz), the thickness of the antibody/antigen monolayer is small compare to the acoustic wave length generated by the sensor.¹² Due to this very thin layer and the high frequency, the antibody/antigen behave like a glassy material, thus the viscoelastic effect is very small and can be neglected. Then, the Sauerbrey equation can be used for the mass calculation. In this study, we were not aimed to precisely determine the surface coverage of protein from the frequency responses. Instead, we used the amplified frequency responses resulted from the enhanced mass changes for increasing the

sensitivity of a protein immunosensor. Previously, various enzyme-based amplification strategies for the detection of enzyme, bacteria, and protein have been reported for increasing the sensitivity.¹³ However, in most cases, single enzyme was used as an enzymatic label and the sensitivities of these QCM immunosensors were not attractive, which need to be improved for the practical application in serum samples.

In the present study, we aimed to increase the QCM immunosensor's sensitivity by enhanced mass amplification strategy through the magnetic bead (MB)-stimulated bienzymatic precipitation of 4-chloro-1-naphthol (CN). For this, MBs (dynabeads[®] Myone[™] Carboxylic acid, 1 μ m diameter, Invitrogen) were used as nanocarriers for attaching numerous, HRP and GOx bienzymes with the secondary antibody (polyclonal interleukin-6 (anti-IL-6, Ab₂) produced in rabbit) (Fig. 1b). We chose MBs as they have high density of COOH groups for covalently attaching numerous bienzymes and Ab₂. Also, MB provides simple and easy separation and purification of the bienzymes-Ab₂ conjugate by magnetic separation. In the presence of glucose and CN, the conjugates generate enormous amounts of benzo-4-chlorocyclohexadienone precipitates that accumulate on the QCM surface resulting in an enhanced mass amplification. The resulting mass enhancement can be detected by monitoring the frequency change, where the magnitude of the frequency change corresponds to the concentration of protein bound to the immunosensor probe. No previous report using magnetic bead-bienzymatic bioconjugates in QCM have attempted for the detection of a protein biomarker through the biocatalytic precipitations. This enhanced mass amplification strategy has been used for the detection of a model multifunctional serum cytokine protein, interleukin-6 (IL-6), which is a biomarker for several types of cancers including head and neck squamous cell carcinoma (HNSCC).¹⁴ The physiological level of IL-6 in healthy individuals is ≤ 6 pg ml⁻¹, whereas its level is over expressed in patient with HNSCC (≥ 20 pg ml⁻¹).¹⁵

Fig. 1 outlines the design of a QCM immunosensor (see ESI† for details) and the principle of the IL-6 detection. Briefly, a gold-coated QCM electrode (8 MHz AT-cut, QCM) was covered with a self-assembled monolayer (SAM) of 3-mercaptopropionic acid (MPA). The uncoated QCM sites were treated with mercaptoethanol. Protein A (PA) was then covalently attached on the MPA-coated QCM electrode through the EDC/NHS coupling reaction, which forms amide bonds between the -COOH and -NH₂ groups of MPA and PA, respectively. Primary monoclonal

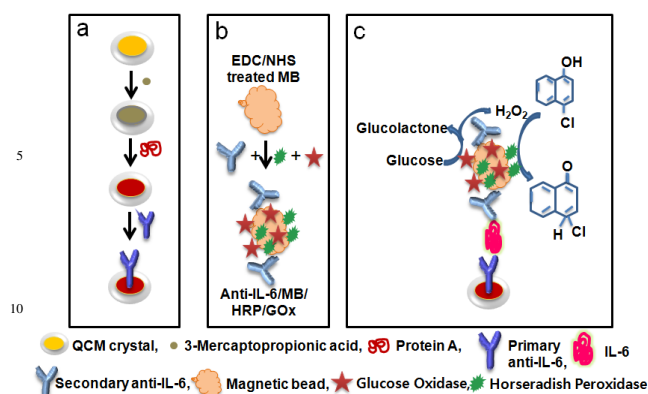


Fig. 1 Schematic illustration of the (a) fabrication of QCM immunosensor, (b) preparation of the bioconjugate, and (c) IL-6 detection principle.

anti-IL-6 antibody (Ab_1) was then immobilized onto the QCM/MPA/PA through the selective interaction between PA and the Fc region of Ab_1 antibody with controlled orientation (Fig. 1a). After washing and blocking the immunosensor surface using 1% bovine serum albumin (BSA), the QCM/MPA/PA/ Ab_1 surface was treated with various concentrations of IL-6 protein in serum. The immunosensor probe was finally fabricated by immunointeracting the Ab_2 /MB/HRP/GOx bioconjugate with the QCM/MPA/PA/ Ab_1 /IL-6 probe. The final QCM/MPA/PA/ Ab_1 /IL-6/ Ab_2 /MB/HRP/GOx (Fig. 1c) probe was assembled into a QCM cell and was connected to an oscillator. Then, the bienzymatic precipitation of CN was followed by introducing an optimum concentration CN and β -glucose in PBS. Frequency responses were continuously measured unless a steady state level was reached. The IL-6 detection was based on the multiple HRP particles induces conversion of CN to benzo-4-chlorocyclohexadienone precipitates in the presence of *in situ* generated H_2O_2 by GOx and glucose, which accumulated on the QCM crystal surface resulted in a dramatic amplification of frequency responses due to the enhanced mass amplification.

The Ab_2 /MB/HRP/GOx bioconjugate was characterized using scanning electron microscopy (SEM) technique. Fig. 2a and 2b show the SEM images obtained for a MB and anti- Ab_2 /MB/HRP/GOx conjugate, respectively. The SEM image of the conjugate clearly shows there are over layers covered the surface of the MB and the brightness of the bare MB surface decreased upon conjugation. The diameter of the MB increased after the Ab_2 /HRP/GOx conjugation, which are uniformly distributed and separated from each other. The increased diameter of the conjugate was further confirmed using the dynamic light scattering (DLS) technique. The hydrodynamic diameter of the conjugate (1250 nm) was found to be increased than that of a bare MB (1119 nm) (Fig. S1, ESI[†]), clearly proved the formation

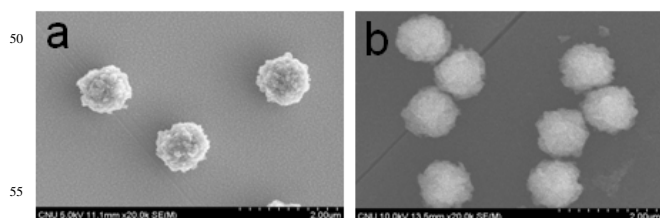


Fig. 2 SEM images of (a) MB and (b) Ab_2 /MB/HRP/GOx conjugates. Insets show the images of bare MB and conjugate.

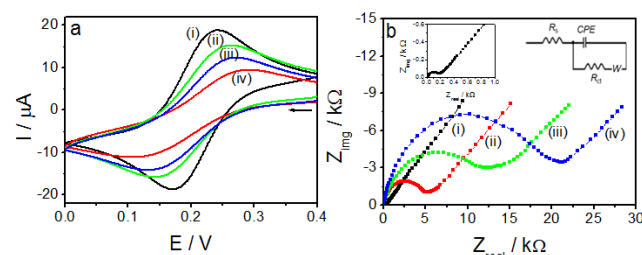


Fig. 3 (a) CVs and (b) Nyquist plots of the EIS spectra for the (i) bare QCM, (ii) QCM/MPA, (iii) QCM/MPA/PA and (iv) QCM/MPA/PA/anti-IL-6 modified electrodes in a 1.0 mM $Fe(CN)_6^{3-/4-}$ solution. Insets show the Nyquist plot of the bare QCM electrode and the equivalent circuit.

of the MB-supported bioconjugate.

The cyclic voltammetry (CV) technique was performed for the characterization of the immunosensor probe at different modification stages. Fig. 3a shows the CVs recorded for various modified electrodes in a $Fe(CN)_6^{3-/4-}$ solution. The CV for a (i) bare QCM electrode exhibited a peak separation (ΔE_p) value of about 0.07 V, indicating a quasi-reversible electron transfer process of $Fe(CN)_6^{3-/4-}$ redox couple. However, the ΔE_p values for (ii) QCM/MPA (0.11V), (iii) QCM/MPA/PA (0.13V) and (iv) QCM/MPA/PA/ Ab_1 (0.16V) modified electrodes showed irreversible processes of $Fe(CN)_6^{3-/4-}$ electron transfer. Additionally, the peak currents (I_p) of the $Fe(CN)_6^{3-/4-}$ electron transfer process significantly decreased as the MPA, PA, and Ab_1 were immobilized on the bare QCM electrode. The increased ΔE_p and decreased I_p values of $Fe(CN)_6^{3-/4-}$ redox reaction for QCM/MPA, QCM/MPA/PA, and QCM/MPA/PA/ Ab_1 modified electrodes indicate that the MPA, PA, and Ab_1 successfully immobilized on the QCM electrode, which acted as barriers for the electron transfer process of $Fe(CN)_6^{3-/4-}$ couple. Electrochemical impedance spectroscopy (EIS)¹⁶ technique provides the information on the surface conductivity and could be used for the characterization of the immunosensor probe at various modification steps in terms of charge transfer resistance (R_{ct}). The R_{ct} value, which exhibits the charge transfer kinetics of the $Fe(CN)_6^{3-/4-}$ redox system could be used to prove the existence of biomolecular layers on the modified electrode. Fig. 3b shows the Nyquist plots of EIS measurements for the bare (i) QCM, (ii) QCM/MPA, (iii) QCM/MPA/PA, and (iv) QCM/MPA/PA/ Ab_1 modified electrodes recorded in a 1.0 mM $Fe(CN)_6^{3-/4-}$ solution. The R_{ct} values were determined from the diameters of the semicircle parts at higher frequencies in the Nyquist plots. The R_{ct} value of a bare QCM crystal (0.2 k Ω) increased to a value of ~6 k Ω , after the attachment of MPA (QCM/MPA), indicating that the MPA was covered on the QCM surface. The further increases in R_{ct} values for QCM/MPA/PA (~15 k Ω) and QCM/MPA/PA/ Ab_1 (~24 k Ω) electrodes clearly revealed the successful immobilizations of PA and Ab_1 on the immunosensor probe.

For achieving the highest sensitivity, two control experiments were performed. Firstly, the non-specific adsorption of the conjugates and the non-specific binding of other biomolecules were examined by measuring the frequency responses during precipitation reaction with the immunosensor probe with or without BSA blocking in PBS and serum samples (Fig. S2, ESI[†]). The results clearly show that the BSA blocking significantly minimized the non-specific adsorption of the conjugates or non-specific binding of other biomolecules in serum samples.

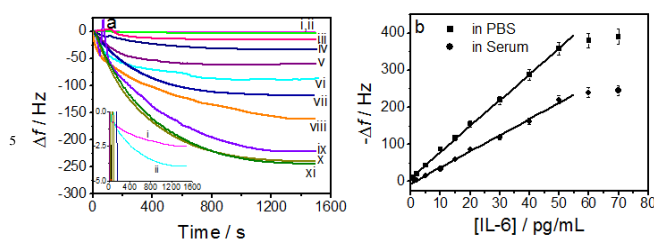


Fig. 4 (a) Frequency responses measured during the precipitation reaction with various concentrations of IL-6 in human serum: (i) 1, (ii) 2, (iii) 5, (iv) 10, (v) 15, (vi) 20, (vii) 30, (viii) 40, (ix) 50, (x) 60, and (xi) 70 pg/mL. Inset shows the responses at two lowest concentrations. (b) Corresponding calibration plot.

Secondly, the frequency response obtained with the anti- $\text{Ab}_2/\text{MB}/\text{HRP}/\text{GOx}$ conjugates was compared with that obtained for only $\text{Ab}_2/\text{HRP}/\text{GOx}$ conjugates without magnetic bead (MB) (Fig.S3, ESI[†]). In the case of $\text{Ab}_2/\text{HRP}/\text{GOx}$ conjugates, the Δf response did not significantly decreased (~ 5 Hz) due to the formation of a less amount of precipitates by the lower amounts of bienzymes in the conjugates. The use of MB increases the amounts of HRP and GOx enzymes in the conjugates, thus enhanced the amount of precipitates formed resulted in a large decrease in Δf response (~ 31 Hz). Thus, the highly sensitive detection of IL-6 through the proposed enhanced mass amplification strategy was evaluated by measuring the Δf response at various spiked IL-6 concentrations in human serum samples (Fig. 4a). As the concentration of IL-6 increased, the Δf responses decreased due to the formation of more precipitates by the larger amount of $\text{Ab}_2/\text{MB}/\text{HRP}/\text{GOx}$ bioconjugates. The linear calibration plot of Δf vs. IL-6 concentrations is shown in Fig. 4b. For a comparison, the calibration plot obtained in PBS is also shown. The Δf responses in human serum samples were about 5% lower than that obtained in PBS. The lower responses obtained were due to the presence of various matrices in serum samples. A linear dynamic range between 1 and 50 pg mL^{-1} concentration of IL-6 was observed. The limit of detection (LOD) was estimated to be 0.6 ± 0.036 pg mL^{-1} ($n = 5$) based on 3 standard deviation units larger than the blank signal. The reproducibility expressed in terms of the relative standard deviation (RSD) was about 6.7% ($n=5$) at 5 pg mL^{-1} of IL-6. The observed LOD of IL-6 is comparable to that of a highly sensitive electrochemical immunosensor (0.5 pg mL^{-1})^{17a} and much lower than that of other IL-6 immunosensors.^{17b,c}

No interferences from the other proteins such as human serum albumin (HSA), prostate specific antigen (PSA), human carcinoembryonic antigen (CEA), human immunoglobulin (IgG), and human thrombin (TB) were observed as the non-specific binding of other proteins were minimized by BSA blocking (Fig. S4, ESI[†]). The stability of the proposed high sensitive QCM IL-6 immunosensor was determined for two months by measuring the response once a time in every two days after regeneration of the sensor surface (see ESI[†] for regeneration step). For six weeks, the Δf responses retained almost 90 % of its initial response (Fig. S5, ESI[†]). These results demonstrated that the proposed enhanced mass amplification strategy based QCM immunosensor hold great promise for IL-6 detection in serum samples with high specificity and stability.

In conclusion, we developed a stimulated mass enhancement amplification strategy based on MB-supported bienzymatic precipitation for a high sensitive detection of IL-6 in serum. The IL-6 detection was based on the measurements of the enhanced decrement of the Δf responses due to the accumulation of enormous amount of precipitates resulted from the biocatalytic precipitation of CN by HRP and GOx in the conjugates. The proposed QCM immunosensor method could be used as a viable technique for the detection of other proteins in serum by simply changing the specific antibody in bioconjugates and in the immunosensor probe.

This research was supported by the Basic Research Program for regional university (2012RIA1A4A01007256) funded by the National Research Foundation, Korean government (MEST) and a Chungnam National University research grant (2014-0693-01).

Graduate School of Analytical Science and Technology, Chungnam National University, Daejeon 305-764, South Korea
 Fax: 82-42-821-8541; Tel: 82-42-821-8546; E-mail: marahman@cnu.ac.kr
[†] Electronic supplementary information (ESI) available: Experimental details, Figs. S1, S2, S3, S4 and S5. See DOI: 10.1039/b000000x/

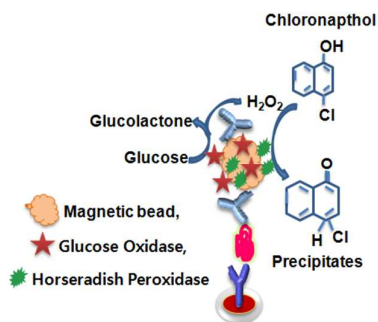
Notes and references

- A. M. Yates, S. J. Elvin and D. E. Williamson, *J. Immunoassay*, 1999, **20**, 31-44.
- M. Teppo and C. P. Maury, *J. Clin. Chem.*, 1987, **33**, 2024-2027.
- T. Li, E.-J. Jo and M.-G. Kim, *Chem. Commun.*, 2012, **48**, 2304-2306.
- Z. F. Fu, F. Yan, H. Liu, Z. J. Yang and H. X. Ju, *Biosens. Bioelectron.*, 2008, **23**, 1063-1069.
- D. S. Reichmuth, S. K. Wang, L. M. Barrett, D. J. Throckmorton, W. Einfeld and A. K. Singh, *Lab Chip*, 2008, **8**, 1319-1324.
- S. H. Hu, S. C. Zhang, Z. C. Hu, Z. Xing and X. R. Zhang, *Anal. Chem.*, 2007, **79**, 923-929.
- (a) C. Liu, T. Lei, K. Ino, T. Matsue, N. Tao and C.-Z. Li, *Chem. Commun.*, 2012, **48**, 10389-10391; (b) S. Krishnan, V. Mani, D. Wasalathanthri, C. V. Kumar and J. F. Rusling, *Angew Chem. Int. Ed.* 2011, **50**, 1175-1178.
- (a) G.-F. Jie, P. Liu and S.-S. Zhang, *Chem. Commun.*, 2010, **46**, 1323-1325; (b) G. Jie, L. Li, C. Chen, J. Xuan and J. Zhu, *Biosens. Bioelectron.*, 2010, **25**, 1781-1788.
- (a) B. S. Munge, A. L. Coffey, J. M. Doucette, B. K. Somba, R. Malhotra, V. Patel, J. S. Gutkind and J. F. Rusling, *Angew Chem. Int. Ed.* 2011, **50**, 7915-7918; (b) K. Chuah, L. M. H. Lai, I. Y. Goon, S. G. Parker and J. J. Gooding, *Chem. Commun.*, 2012, **48**, 3503-3505.
- (a) D. Tang, R. Yuan, Y. Chai, *Analyst*, 2008, **133**, 933-938; (b) S. M. Knudsen, J. Lee, A. D. Ellington, and C. A. Savran, *J. Am. Chem. Soc.*, 2006, **128**, 15936-15937.
- G. Sauerbrey, *Z. Phys.* 1959, **155**, 206-222.
- S. P. Sakti, P. Hauptmann, B. Zimmermann, F. Buhling and S. Ansorge, *Sens. Actuators, B*, 2001, **78**, 257-262.
- (a) R. C. Ebersole and M. D. Ward, *J. Am. Chem. Soc.*, 1988, **110**, 6494-6498; (b) C. Ruan, K. Zeng, O. K. Varghese and C. A. Grimes, *Anal. Chem.*, 2003, **75**, 6494-6498; (c) J. Zhou, N. Gan, T. Li, H. Zhou, X. Li, Y. Cao, L. Wang, W. Sang and F. Hu, *Sens. Actuators, B*, 2013, **178**, 494-500.
- T. Kishimoto, *Annu. Rev. Immunol.* 2005, **23**, 1-21.
- D. S. Hong, L. S. Angelo, and R. Kurzrock, *Cancer* 2007, **110**, 1911-1928.
- A. J. Bard and L. R. Faulkner, *Electrochemical Methods: Fundamentals and Applications*, John Wiley & Sons Inc., New York, 2nd edn., 2001.
- (a) R. Malhotra, V. Patel, J. P. Vaque, J. S. Gutkind and J. F. Rusling, *Anal. Chem.* 2010, **82**, 3118-3123; (b) B. V. Chikkaveeraiiah, A. Bhirde, R. Malhotra, V. Patel, J. S. Gutkind and J. F. Rusling, *Anal. Chem.* 2009, **81**, 9129-9134; (c) B. S. Munge, C. E. Crause, R. Malhotra, V. Patel, J. S. Gutkind and J. F. Rusling, *Electrochem. Commun.* 2009, **11**, 1009-1012.

Table of Contents

Stimulated mass enhancement strategy-based highly sensitive detection of a protein in serum using quartz crystal microbalance technique†

Rashida Akter, Bongjin Jeong and Md. Aminur Rahman *



Quartz crystal microbalance immunosensor for highly sensitive detection of interleukin-6 in serum using magnetic bead-supported-byenzymes catalyzed stimulated mass enhancement strategy.